Compression and broadening of phase-conjugate pulses in photorefractive self-pumped phase conjugators

Changxi Yang and Min Xiao

Department of Physics, University of Arkansas, Fayetteville, Arkansas 72701

Malgosia Kaczmarek

School of Physics, University of Exeter, Exeter EX4 4QL, UK

Received December 9, 1999; revised manuscript received April 24, 2000

Pulse propagation and shaping are investigated in photorefractive self-pumped phase conjugators in both transmission- and reflection-grating regimes. The dispersion properties of self-pumped phase conjugators are analyzed by taking into account both the grating dispersion and the angular dispersion. The complex transfer functions are obtained by treating the crystal as a linear dispersive medium. We show that the pulse width as a result of the self-pumped phase conjugation is much wider in the reflection regime than in the transmission regime. The experimental results are consistent with the results calculated for the transmission-grating regime, indicating that this type grating is the dominant mechanism in the case of a femtosecond self-pumped phase conjugator. © 2000 Optical Society of America [S0740-3224(00)00908-5]

OCIS codes: 190.5040, 190.5330, 190.5530, 320.5520.

1. INTRODUCTION

Pulse propagation in dispersive media, especially in optical fibers, has been extensively studied and is governed by the combined effects of group-velocity dispersion (GVD) and nonlinear effects.[1–3] In the anomalous-dispersion regime the combined effects of GVD and nonlinear effects can give rise to the generation of optical solitons in a fiber.[4] Recently, pulse propagation in periodic media with strong dispersion in and around the stop band, such as fiber gratings, has attracted considerable attention.[5–11] Winful[12] proposed the application of a fiber grating for correction of a nonlinear chirp to compress a pulse in a long-transmission fiber grating. Russell[13] pointed out that gratings exhibit strong dispersion for the frequencies close to the Bragg resonance. This dispersion is due to the strong frequency dependence of the group velocity of light propagating through a grating. Eggleton *et al.*[14,15] reported the generation of Bragg solitons in optical fiber gratings, which rely on the strong GVD provided by the Bragg grating at the bandgap edge.

Propagation of light through gratings in photosensitive materials (such as photorefractive crystals) has also attracted a lot of research.[16,17] However, the effect of dispersion on the incident pulse propagation has not been sufficiently well modeled, for example, in configurations such as the self-pumped phase conjugator. Since dispersion determines the temporal profile of the self-pumped phase-conjugate pulse, all components contributing to the magnitude of dispersion, such as grating dispersion, angular dispersion, and the intrinsic dispersion of the material, have to be taken into account.

Femtosecond self-pumped phase conjugation (SPPC) at various wavelengths has been observed in $BaTiO_3$.[18–23] But its temporal characteristics have not been investigated yet. Although Yariv *et al.*[24] proposed that the process of nonlinear optical phase conjugation could be utilized to compensate for channel dispersion, they discussed only the phase conjugation achieved by four-wave mixing in nondispersive media. In this paper we explore the effect of the dispersion in a self-pumped phase-conjugate mirror (SPPCM) on the temporal characteristics of femtosecond SPPC, taking account of the grating dispersion and the angular dispersion.

Photorefractive SPPC is generated by certain gratings formed by the pump and the fanning beams. Owing to the slow response time of a photorefractive crystal, for instance, $BaTiO_3$, the grating is formed by the accumulating effect of a number of pulses. In this paper we will therefore consider only the steady-state case and take into account the linear pulse compression and chirp compensation.

Generally, transmission gratings, reflection gratings, and $2k$ gratings may all coexist in SPPCM.[25] There are two typical configurations of SPPCM's. In the first one, a transmission grating dominates both a reflection grating and a $2k$ grating.[26] We will call it transmission-grating-based SPPCM (TG-SPPCM) [see Fig. 1(a)]. In the other configuration a reflection grating dominates a transmission grating. We will call it a reflection-grating-based SPPCM (RG-SPPCM).[27,28] $2k$-grating based SPPCM [see Fig. 1(b)] can be considered as a special case of the RG-SPPCM.[29]

In Section 2 we analyze the dispersion properties of the TG-SPPCM and the RG-SPPCM. In Section 3 we introduce the complex transfer functions for the two SPPCM configurations. In Section 4 the femtosecond SPPC's

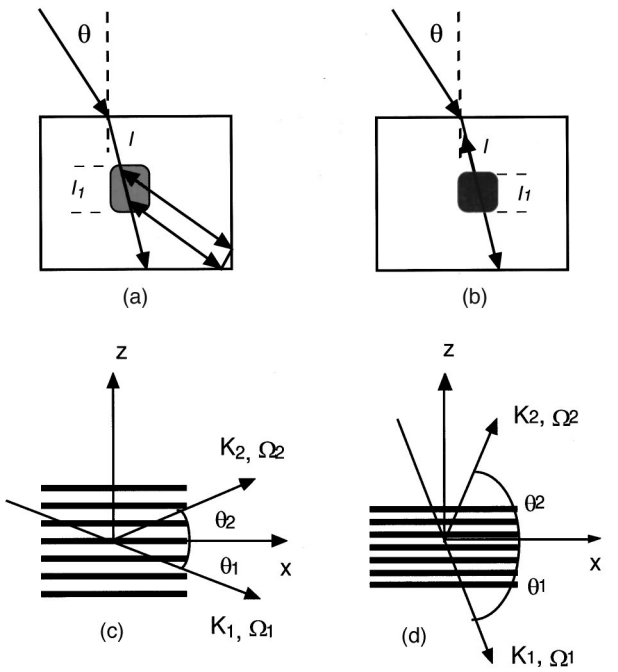

Fig. 1. (a) Transmission-grating-based self-pumped phase conjugator; (b) reflection-grating-based self-pumped phase conjugator; (c) transmission grating; (d) reflection grating. (K_1, Ω_1) indicate the incident beam; (K_2, Ω_2) indicate the diffracted beam; $\theta_{1,2}$ are the incident and the diffracted angles. l_1 and l are the thickness of grating and the distance between the crystal surface and the grating, respectively. θ is the incident angle in air.

from the TG-SPPCM and the RG-SPPCM are presented, including the case of unchirped and chirped Gaussian pulses. The final two sections (5 and 6) are devoted to the detailed discussion of the results and conclusions.

2. DISPERSION OF SELF-PUMPED PHASE-CONJUGATE MIRRORS

For simplicity we consider that a SPPCM consists of only one grating, which is formed by the central-frequency component of the pump and its fanning beam. The linear refractive index n for a uniform grating is written as $n = n_0 + n_1 \cos Kz$, where n_0 is the average index of refraction of the crystal; n_1 is the amplitude of the refractive-index modulation; and K is the grating wave number along the z axis.

The electric field of the incident (A_1) and diffracted (A_2) waves can be written as

$$E = A_1 \exp[i(\omega t - k_{1x}x - k_{1z}z)] + A_2 \exp[i(\omega t - k_{2x}x - k_{2z}z)] + \text{c.c.}, \quad (1)$$

where $k_{jx,z}$ $(j = 1, 2)$ are the x and the z components of the wave vectors k_j, respectively, and they are related by [see Figs. 1(c) and 1(d)]

$$k_{jx} = k_j \cos\theta_j, \quad k_{jz} = k_j \sin\theta_j \quad (j = 1, 2), \quad (2)$$

where $\theta_{1,2}$ are the incident and the diffracted angles, respectively.

A. Dispersion of the Transmission-Grating-Based Self-Pumped Phase-Conjugate Mirror

For the case of a transmission grating as shown in Fig. 1(c), the amplitudes A_1 and A_2 are assumed to be functions of x only. In order to solve the two-beam coupling equations, we apply the boundary condition that requires[30]

$$k_2(\Omega)\sin\theta_2(\Omega) = k_1 \sin\theta_1 \pm K, \quad (3)$$

where $K = 2\pi/\Lambda$ is the grating wave vector and Λ is the grating period. k_1, θ_1, and K are constants.

From Eq. (3) the first-order derivative of the diffracted angle θ_2 with respect to the frequency Ω is

$$\frac{d\theta_2}{d\Omega} = -\frac{\tan\theta_2}{k_2}\frac{dk_2}{d\Omega}. \quad (4)$$

The phase mismatch is given by

$$\Delta\alpha(\Omega) = k_2(\Omega)\cos\theta_2(\Omega) - k_1\cos\theta_1. \quad (5)$$

We expand $\Delta\alpha$ at the center frequency of the pulse ω_1 as $\Delta\alpha(\Omega) = \Sigma_0^\infty \alpha_n(\Omega - \omega_l)^n$ with the expansion coefficients $\alpha_n = (1/n!)d^n\Delta\alpha(\Omega)/d\Omega^n|_{\omega_l,\theta_B}$, where θ_B is the Bragg angle.

The phase-matching condition requires $\alpha_0 = 0$. Using Eqs. (4) and (5) the first- and second-order coefficients of $\Delta\alpha$ can be obtained:

$$\alpha_1 = \frac{1}{\cos\theta_2}\frac{dk_2}{d\Omega}\bigg|_{\omega_l,\theta_B}, \quad (6)$$

$$\alpha_2 = \left[-\frac{\tan^2\theta_2}{2k_2\cos\theta_2}\left(\frac{dk_2}{d\Omega}\right)^2 + \frac{1}{2\cos\theta_2}\frac{d^2k_2}{d\Omega^2}\right]\bigg|_{\omega_l,\theta_B}, \quad (7)$$

where $k' = dk/d\Omega$ and $k'' = d^2k/d\Omega^2$ are the group velocity and the GVD of the crystal, respectively. The first- and second-order dispersion of the grating, α_1 and α_2, are functions of the material dispersion. Just as material dispersion does, grating dispersion makes the diffracted beams (of different frequencies) have different group velocities.

B. Dispersion of the Reflection-Grating-Based Self-Pumped Phase-Conjugate Mirror

In the case of a reflection grating as shown in Fig. 1(d), the amplitudes A_1 and A_2 are assumed to be functions of z only. The boundary condition and phase mismatch[30] are, respectively,

$$k_2(\Omega)\cos\theta_2(\Omega) - k_1\cos\theta_1 = 0, \quad (8)$$

$$\Delta\beta(\Omega) = k_2(\Omega)\sin\theta_2(\Omega) - k_1\sin\theta_1 \pm K. \quad (9)$$

Similarly to the case of the transmission grating, we obtain

$$\frac{d\theta_2}{d\Omega} = \frac{1}{k_2\tan\theta_2}\frac{dk_2}{d\Omega}, \quad (10)$$

$$\beta_1 = \frac{1}{\sin\theta_2}\frac{dk_2}{d\Omega}\bigg|_{\omega_l,\theta_B}, \quad (11)$$

$$\beta_2 = \left[-\frac{1}{2k_2 \sin\theta_2 \tan^2\theta_2}\left(\frac{\mathrm{d}k_2}{\mathrm{d}\Omega}\right)^2 + \frac{1}{2\sin\theta_2}\frac{\mathrm{d}^2k_2}{\mathrm{d}\Omega^2}\right]\Bigg|_{\omega_l,\theta_B}. \quad (12)$$

β_1 and β_2 are the first- and second-order dispersion of the reflection grating.

C. Angular Dispersion of Self-Pumped Phase-Conjugate Mirrors

The angular dispersion is induced by the refraction at the air–crystal interface, the diffraction from the gratings, and the phase changes at the total internal surface reflections in SPPCM. The angular dispersion for a SPPCM is given by[31]

$$b_2 = -\frac{4\lambda^3}{2\pi c^2}\left[\frac{l_1 \sin^2\theta}{n_0^2(n_0^2 - \sin^2\theta)}\left(\frac{\mathrm{d}n_0}{\mathrm{d}\lambda}\right)^2 + \frac{L}{(2n_0\Lambda\cos\theta_B)^2}\left(1 - \frac{\lambda}{n_0}\frac{\mathrm{d}n_0}{\mathrm{d}\lambda}\right)^2 + \frac{l_4 \sin^2\theta}{(n_0\cos\theta)^2}\left(\frac{\mathrm{d}n_0}{\mathrm{d}\lambda}\right)^2\right], \quad (13)$$

where l_1 is the distance between the grating and the crystal surface (see Fig. 1), L is the pulse propagation distance inside the crystal, θ is the incident angle in air, θ_B is the Bragg angle of the grating inside the crystal, and l_4 is the SPPC propagation distance in air. For Bragg angles where $0 < \theta_B < 45°$, b_2 represents the angular dispersion of the TG-SPPCM. For Bragg angles where $45° < \theta_B < 90°$, b_2 represents the angular dispersion of the RG-SPPCM.

3. COMPLEX TRANSFER FUNCTIONS OF SELF-PUMPED PHASE-CONJUGATE MIRRORS

We neglect the self-phase modulation and the cross-phase modulation by treating the crystal as a linear dispersive medium. The SPPCM can be represented by a complex transfer function in the frequency domain[2]: $H(\Omega) = R(\Omega)\exp[-i\Psi(\Omega)]$, where $R(\Omega)$ is the amplitude response and $\Psi(\Omega)$ is the phase response. $\Psi(\Omega)$ can be expanded as $\Psi(\Omega) = \Sigma_0^\infty b_n(\Omega - \omega_l)^n$, where $b_n = (1/n!)\mathrm{d}^n\Psi(\Omega)/\mathrm{d}\Omega^n|_{\omega_l}$ and ω_l is the center frequency of the pulse.

Using the coupled-mode theory and the nondepleted-pump approximation, we can obtain the diffraction from the transmission grating[30]:

$$R(\Omega) = {R_0}^T \exp[il\Delta\alpha(\Omega)/2]\sin c[l\Delta\alpha(\Omega)/2], \quad (14)$$

where ${R_0}^T$ is a complex constant and l is the thickness of the transmission grating. Near the phase-matching condition, i.e., $l\Delta\alpha(\Omega) \ll 1$, we have

$$\sin c[l\Delta\alpha(\Omega)/2] \approx \exp\{-(1/6)[l\Delta\alpha(\Omega)/2]^2\}. \quad (15)$$

We neglect the cubic and higher-order terms in the expansions, and the complex transfer function of the TG-SPPCM is found to be

$$H^T(\Omega) = {R_0}^T \exp\left\{-ib_0 + i\left(\frac{l\alpha_1}{2} - b_1\right)\Omega + i\left[\frac{l^2{\alpha_1}^2}{24} + i\left(\frac{l\alpha_2}{2} - b_2\right)\right]\Omega^2\right\}. \quad (16)$$

Similarly, the complex transfer function of the RG-SPPCM is given by

$$H^R(\Omega) = {R_0}^R \exp\left\{-ib_0 + i\left(\frac{l\beta_1}{2} - b_1\right)\Omega + i\left[\frac{l^2{\beta_1}^2}{24} + i\left(\frac{l\beta_2}{2} - b_2\right)\right]\Omega^2\right\}. \quad (17)$$

4. FEMTOSECOND SELF-PUMPED PHASE CONJUGATION WITH TRANSMISSION AND REFLECTION GRATINGS

Once the transfer function is obtained, the time-dependent SPPC field can be expressed as[1,2]

$$E_{pc}(z,T) = \frac{1}{2\pi}\int_{-\infty}^{\infty} H(\Omega)E(0,\Omega) \times \exp(-i\Omega T)\exp\left(-i\frac{k''z}{2}\Omega^2\right)\mathrm{d}\Omega, \quad (18)$$

where z is the pulse propagation distance inside the crystal and $E(0,\Omega)$ is the Fourier transform of pump pulse $E(0,T)$.

A. Self-Pumped Phase Conjugation of Unchirped Gaussian Pulses from the Transmission-Grating-Based Self-Pumped Phase-Conjugate Mirror

We consider pump pulses of unchirped Gaussian shape,[1] e.g., $E(0,T) = \exp(-T^2/2{T_0}^2)$ and in the frequency domain the incident field can be written as $E(0,\Omega) = \sqrt{2\pi}T_0\exp(-T_0^2\Omega^2/2)$. Inserting Eq. (16) and $E(0,\Omega)$ into Eq. (18), the SPPC field is obtained:

$$E_{pc}(z,T) = |E_{pc}|\exp[-(T + T_c)^2/2{T_1}^2 + \phi(z,T)], \quad (19)$$

where $|E_{pc}|$ is the amplitude of the SPPC field, T_c is a constant that leads to a shift of the pulse on the time axis, T_1 is the half-width (at the $1/e$ intensity point), and ϕ is the time-dependent phase.

Owing to the dispersion of the SPPCM, although the SPPC pulse broadens, it still maintains the Gaussian shape. The broadening factor of the SPPC pulse width is given by

$$\frac{T_1}{T_0} = \left(1 + \frac{l^2{\alpha_1}^2}{12{T_0}^2}\right)^{1/2}\left\{1 + \left[\frac{2b_2 + k''z - l\alpha_2}{{T_0}^2(1 + l^2{\alpha_1}^2/12{T_0}^2)}\right]^2\right\}^{1/2}. \quad (20)$$

The time-dependent phase of the SPPC field is given by

$$\phi(z,T) = \frac{(2b_2 + k''z - l\alpha_2)(T + b_1 - l\alpha_1/2)^2}{2T_0^4\left[\left(1 + \frac{l^2\alpha_l^2}{12T_0^2}\right) + \left(\frac{2b_2 + k''z - l\alpha_2}{T_0^2}\right)^2\right]} - \frac{1}{2}\tan^{-1}\frac{(2b_2 + k''z - l\alpha_2)/T_0^2}{\left(1 + \frac{l^2\alpha_1^2}{12T_0^2}\right)} - b_0. \quad (21)$$

The dispersion-induced chirp is given by

$$\delta\omega = \frac{\partial\phi}{\partial T} = \frac{(2b_2 + k''z - l\alpha_2)(T + b_1 - l\alpha_1/2)}{T_0^4\left[\left(1 + \frac{l^2\alpha_1^2}{12T_0^2}\right) + \left(\frac{2b_2 + k''z - l\alpha_2}{T_0^2}\right)^2\right]}. \quad (22)$$

B. Self-Pumped Phase Conjugation of Chirped Gaussian Pulses from the Transmission-Grating-Based Self-Pumped Phase-Conjugate Mirror

For the case of linearly chirped Gaussian pulses, the incident field can be written as[1] $E(0,T) = \exp[-(1 + iC)T^2/2T_0^2]$, where C is a chirp parameter. The pump pulse is upchirped if $C > 0$ and downchirped if $C < 0$. The unchirped pulses correspond to $C = 0$.[1]

The broadening factor of the SPPC pulse is given by

$$\frac{T_1}{T_0} = \frac{1}{\sqrt{1 + C^2}}\left\{1 + \left[\frac{l^2\alpha_1^2(1 + C^2)}{12T_0^2}\right]\right\}^{1/2}\left[1 + \frac{[2b_2 + k''z - l\alpha_2 - CT_0^2/(1 + C^2)]^2}{[T_0^2/(1 + C^2)]^2[1 + l^2\alpha_1^2(1 + C^2)/12T_0^2]^2}\right]^{1/2}. \quad (23)$$

The time-dependent phase of the SPPC field is

$$\phi(z,T) = \frac{1}{2}\frac{[2b_2 + k''z - l\alpha_2 - CT_0^2/(1 + C^2)](T + b_1 - l\alpha_1/2)^2}{[T_0^2/(1 + C^2) + l^2\alpha_1^2/12]^2 + [2b_2 + k''z - l\alpha_2 - CT_0^2/(1 + C^2)]^2} - \frac{1}{2}\tan^{-1}\frac{2b_2 + k''z - l\alpha_2 - CT_0^2/(1 + C^2)}{T_0^2/(1 + C^2) + l^2\alpha_1^2/12} + \text{const}, \quad (24)$$

and the dispersion-induced chirp is

$$\delta\omega = \frac{[2b_2 + k''z - l\alpha_2 - CT_0^2/(1 + C^2)](T + b_1 - l\alpha_1/2)}{[T_0^2/(1 + C^2) + l^2\alpha_1^2/12]^2 + [2b_2 + k''z - l\alpha_2 - CT_0^2/(1 + C^2)]^2}. \quad (25)$$

From Eqs. (21) and (24) we note that the phase of the SPPC field depends on time, which implies that the instantaneous frequency of the SPPC pulse differs across the pulse from the central frequency ω_l. The SPPC pulse becomes linearly chirped even when the pump is unchirped. The sign of the linear chirp depends on the sign of the net dispersion of the self-pumped phase conjugator. For an unchirped pump pulse, when $2b_2 + k''z - l\alpha_2 > 0$, the SPPC pulse is upchirped ($\delta\omega > 0$), while the opposite occurs when $2b_2 + k''z - l\alpha_2 < 0$.[1] For the chirped pump pulse, when $2b_2 + k''z - l\alpha_2 - CT_0^2/(1 + C^2) > 0$, the SPPC pulse is upchirped ($\delta\omega > 0$), while the opposite occurs when $2b_2 + k''z - l\alpha_2 - CT_0^2/(1 + C^2) < 0$. The SPPC pulse becomes transform limited if $2b_2 + k''z - l\alpha_2 - CT_0^2/(1 + C^2) = 0$.

Following the procedures similar to the case of the TG-SPPCM, we can obtain the broadening factors, the time-dependent phases, and the dispersion-induced chirps of the SPPC pulses from the RG-SPPCM. From Eqs. (16) and (17) we note that the transfer function of the RG-SPPCM has the same form as that of the TG-SPPCM. We can apply the results of the TG-SPPCM to the RG-SPPCM with α_i replaced by $\beta_i (i = 1, 2)$.

5. RESULTS

The chromatic dispersion properties of $BaTiO_3$ are well known, and its refractive index is approximated by the Sellmeier equation.[32] Since only the extraordinarily polarized light generates SPPC's in most photorefractive crystals, in the following calculations we consider the extraordinary refractive index and its derivatives with respect to the frequency. The pump pulse width is assumed as $T_0 = 100$ fs. The thickness of the gratings is $l = 15\,\mu$m, and the propagation distance in the crystal is $z = 10$ mm. The incident angle is $\theta = 45°$ in air.

Figure 2(a) shows the first-order dispersion k', α_1, and β_1 as functions of wavelength. The Bragg angle for the TG-SPPCM is chosen as $2\theta_B = 45°$, and the Bragg angle for the RG-SPPCM is $2\theta_B = 120°$. Figure 2(b) shows α_1 and β_1 versus the Bragg angle at two wavelengths: 450 and 800 nm. Since we assume that the pump wavelength is fixed, the grating period changes accordingly as the Bragg angle changes. We note that as the angle increases, the first-order dispersion of the transmission grating increases, whereas the opposite occurs for the reflection grating.

Figure 3(a) shows the second-order dispersion k'', α_2, and β_2 versus wavelength for four grating periods. Figure 3(b) shows α_2 and β_2 as functions of the Bragg angle for two wavelengths. We note that α_2 and β_2 are larger at 450 nm than at 800 nm, indicating a larger dispersion at a shorter wavelength. This is due to the material dispersion that is higher at shorter wavelengths. α_2 and β_2 equal zero at appropriate Bragg angles for both wavelengths.

Figures 4 and 5 show the broadening factor of the

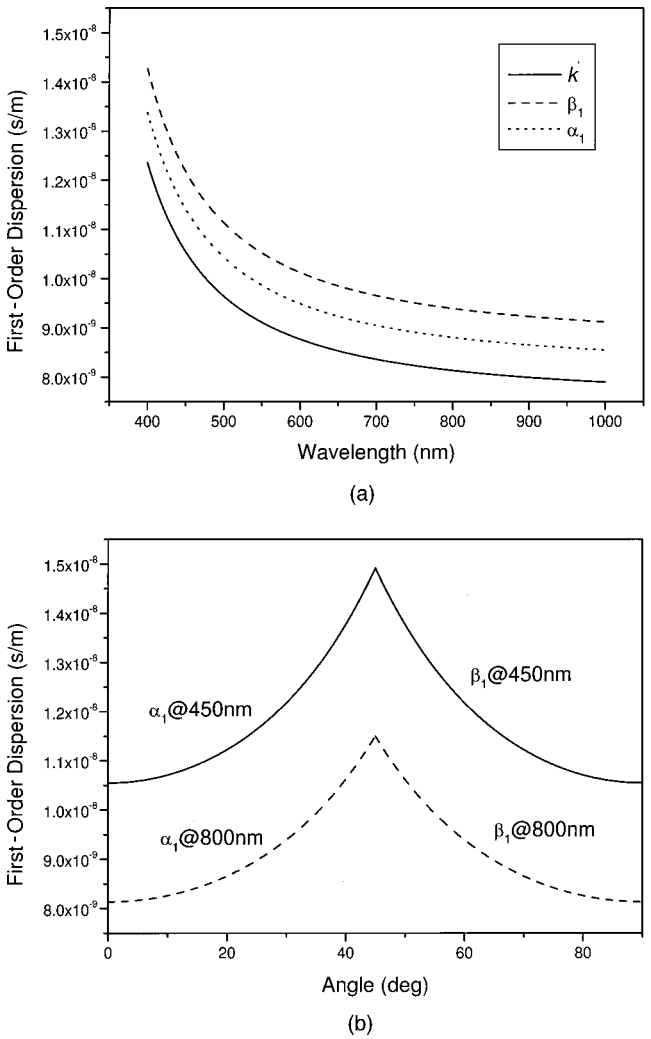

Fig. 2. (a) First-order dispersion k', α_1, and β_1 versus the wavelength. Solid, dashed, and dotted curves represent k', α_1, and β_1, respectively. The Bragg angles are 22.5° and 60° for the transmission and the reflection gratings, respectively. (b) α_1 and β_1 versus the Bragg angle at 450 and 800 nm.

SPPC pulse from the TG-SPPCM versus the grating period for chirped pulses at 450 and 800 nm, respectively. We note that the SPPC pulse of the unchirped Gaussian pulse ($C = 0$) has a smaller broadening factor than the SPPC's of chirped pulses ($C = 1$ and $C = -1$) have at 450 nm. The SPPC pulses broaden for all three values of C at 450 nm. However, the SPPC pulses at 800 nm could be compressed for some grating periods in the case of chirped pump pulses. For example, the SPPC pulses are compressed in the regime of $485\,\text{nm} < \Lambda < 800\,\text{nm}$ for $C = -1$ and $\Lambda > 825\,\text{nm}$ for $C = 1$.

As mentioned above, all three components of dispersion (grating, angular, and material) contribute to its value. We showed that for the SPPC configuration the angular dispersion is negative, while the grating dispersion can be either positive or negative, depending on the experimental conditions. The GVD of a photorefractive crystal is positive. When the GVD of the crystal is canceled by the angular dispersion, then the grating dispersion yields a SPPC pulse with a minimum width. In the transmission-grating geometry and with the pump being an unchirped Gaussian pulse, the SPPC pulse width becomes minimum at $2b_2 + k''z - l\alpha_2 = 0$. This minimum width is given by

$$T_{pc}^{\min} = (1 + l^2\alpha_1^2/12T_0^2)^{1/2}T_0. \tag{26}$$

For a chirped Gaussian pulse the SPPC pulse width becomes minimum at $2b_2 + k''z - l\alpha_2 - CT_0^2/(1 + C^2) = 0$ and is given by

$$T_{pc}^{\min} = [1 + l^2\alpha_1^2(1 + C^2)/12T_0^2]^{1/2}T_0/\sqrt{1 + C^2}. \tag{27}$$

The SPPC pulse becomes, therefore, transform limited and compressed compared with the pump pulse. The minimum pulse widths of SPPC's from the RG-SPPCM have the same forms as Eqs. (26) and (27) with α_1 replaced by β_1.

We note that the minimum pulse width of the SPPC of the unchirped Gaussian pulse is larger than the pump pulse width. However, the minimum pulse width of the SPPC of chirped Gaussian pulses may be smaller than the pump pulse width. From Eqs. (26) and (27) we also note that the minimum SPPC width is determined by the

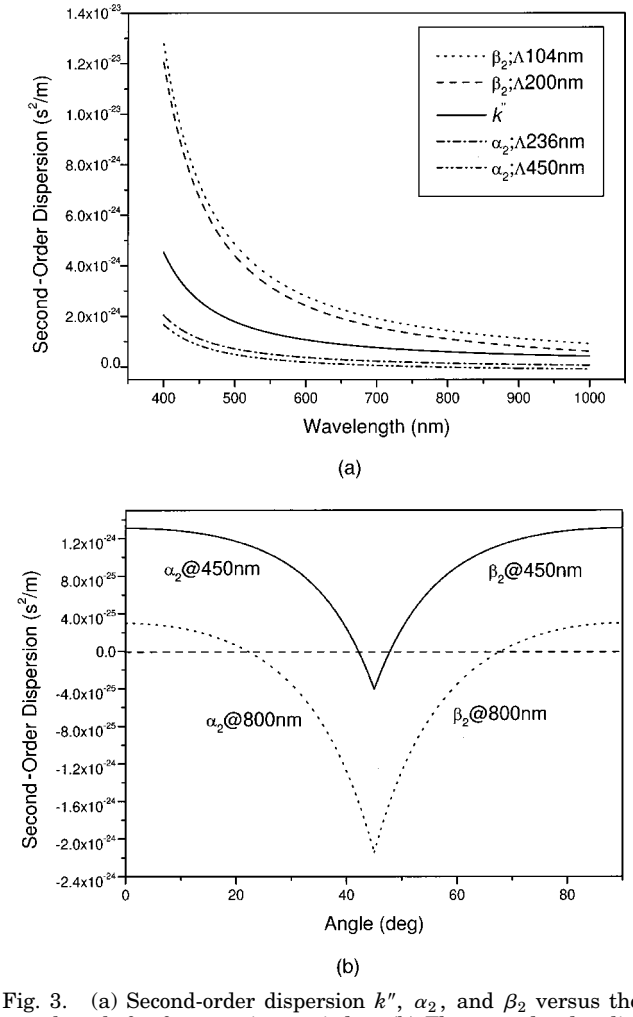

Fig. 3. (a) Second-order dispersion k'', α_2, and β_2 versus the wavelength for four grating periods. (b) The second-order dispersion α_2 and β_2 versus Bragg angle for two wavelengths. The second-order dispersion of the grating changes sign at the zero-dispersion angle θ_D.

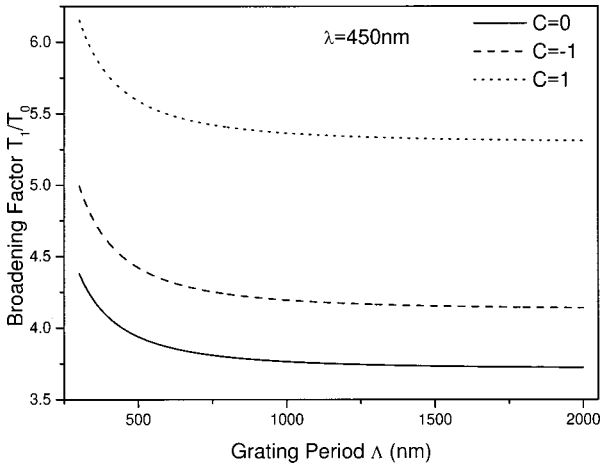

Fig. 4. Broadening factor of the SPPC from the TG-SPPCM at 450 nm versus the grating period. Solid, dashed, and dotted curves represent the chirp parameter $C = 0, -1, 1$, respectively. The SPPC's broaden for the three cases.

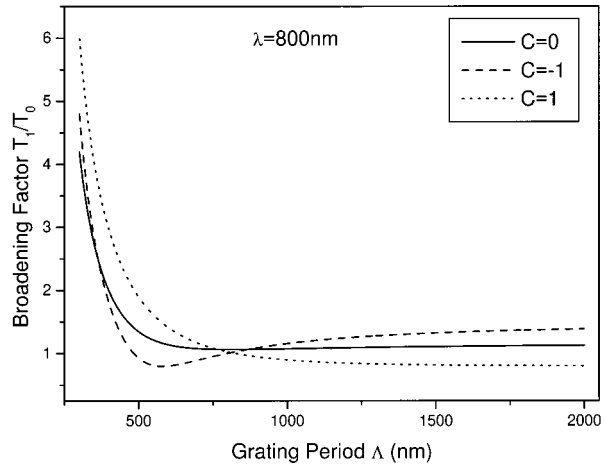

Fig. 5. Broadening factor of the SPPC from the TG-SPPCM at 800 nm versus the grating period. Solid, dashed, and dotted curves represent the chirp parameter $C = 0, -1, 1$, respectively. The SPPC is compressed in the regimes of $485\,\text{nm} < \Lambda < 800\,\text{nm}$ for $C = -1$ and $\Lambda > 825\,\text{nm}$ for $C = 1$.

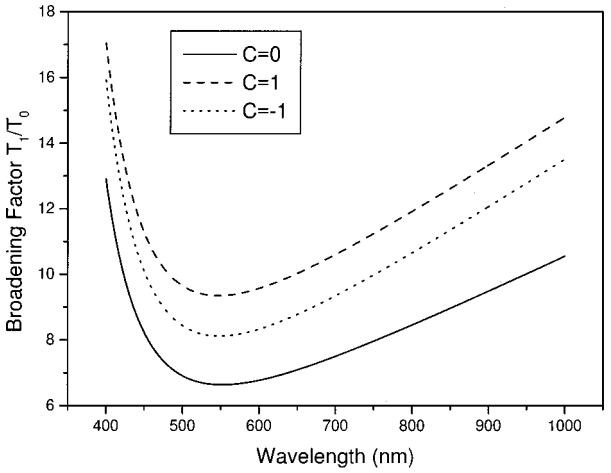

Fig. 6. Broadening factor of the SPPC from the $2k$-grating versus the wavelength for three chirp parameters. The period of the $2k$ grating relates to the wavelength as $\Lambda = \lambda/2n_0$.

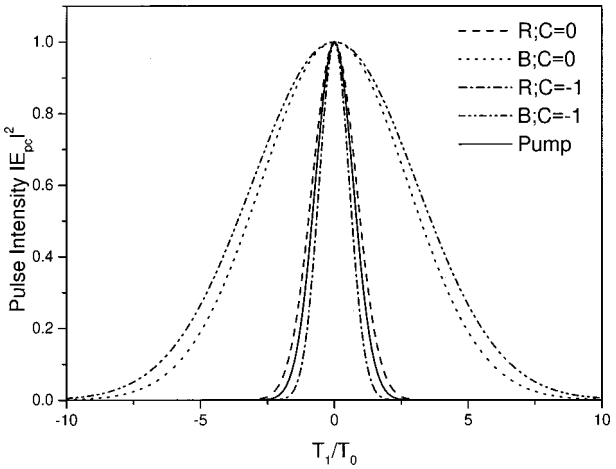

Fig. 7. Pulse shapes of SPPC's from the TG-SPPCM at 450 and 800 nm for two chirp parameters. The solid curve represents a pump pulse of unchirped Gaussian shape. Dashed (R) and dashed-dotted (R) curves are the SPPC pulse shapes at 800 nm for $C = 0$ and $C = -1$, respectively. Dotted (B) and dashed-dotted-dotted (B) curves are the SPPC pulse shapes at 450 nm for $C = 0$ and $C = -1$, respectively. The SPPC pulse at 800 nm with $C = -1$ is compressed.

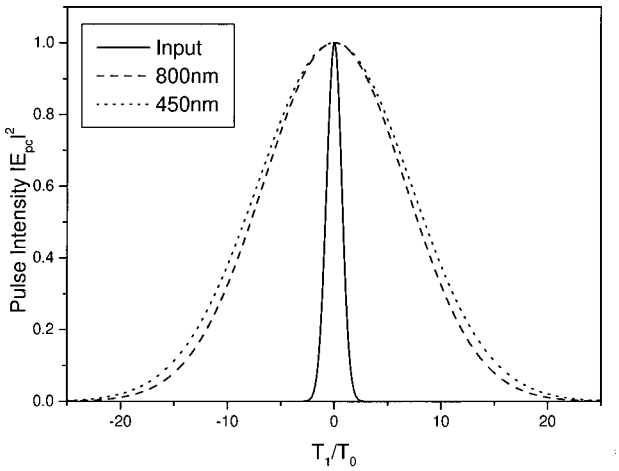

Fig. 8. Pulse shapes of SPPC from $2k$-grating-based SPPCM. Solid, dashed, and dotted curves represent the pump pulse, SPPC at 800 nm, and SPPC at 450 nm, respectively.

first-order dispersion of the grating. The diffraction from the grating rapidly varies with the frequency detuning, which reduces the effective bandwidth of the diffracted pulses. This reduction of bandwidth of diffracted pulses results in the temporal broadening of the SPPC pulse.

Figure 6 shows the broadening factors of the SPPC pulses from the $2k$-grating based SPPCM versus wavelength. The grating period relates to wavelength as $\Lambda = \lambda/2n_0$. Comparing the results from Figs. 4, 5, and 6, we can see that the broadening factor in the $2k$ grating based SPPCM is much larger than that of the TG-SPPCM.

Compared with the transmission grating, the $2k$ grating exhibits large angular dispersion because of its small grating period. The net dispersion of $2k$-grating based SPPCM is larger than that of the transmission grating, which leads to the larger broadening factors of the SPPC pulse shown in Fig. 6.

As examples, we show the pulse shapes of the SPPC's from the TG-SPPCM and the $2k$-grating based SPPCM in Figs. 7 and 8, respectively. Figure 7 shows the SPPC pulse shapes of the unchirped and chirped Gaussian pump pulses from the TG-SPPCM at 450 and 800 nm. The grating period is assumed as $\Lambda = 580\,\text{nm}$ for the two pump wavelengths. For unchirped Gaussian pump pulses ($C = 0$) their SPPC pulses are broadened. The broadening factors are 1.16 and 3.88 for 800 and 450 nm, respectively. When the 800-nm pump is downchirped ($C = -1$), the SPPC pulse is compressed with a compression factor of 0.8. However, for the chirped 450-nm pulse, broadening with a factor of 4.34 occurs.

Figure 8 shows the pulse shapes of the SPPC's from the $2k$-grating based SPPCM at 450 and 800 nm. The broadening factors are 9.42 and 10.15 for 800 and 450 nm, respectively.

6. DISCUSSION AND CONCLUSIONS

From Fig. 5 we note that the second-order dispersion of the grating changes sign as the Bragg angle changes. The grating exhibits zero second-order dispersion when the Bragg angle satisfies

$$\theta_D{}^T = \tan^{-1}\sqrt{(\mathrm{d}^2k/\mathrm{d}\Omega^2)/[k(\mathrm{d}k/\mathrm{d}\Omega)^2]} \tag{28}$$

for the transmission grating and

$$\theta_D{}^R = \cot^{-1}\sqrt{(\mathrm{d}^2k/\mathrm{d}\Omega^2)/[k(\mathrm{d}k/\mathrm{d}\Omega)^2]} \tag{29}$$

for the reflection grating.

The wavelength at which the GVD equals zero is referred to as the zero-dispersion wavelength in fiber optics.[1] Similarly we may call the angle at which the grating shows zero second-order dispersion as zero-dispersion angle θ_D. Figure 9 shows θ_D versus wavelength for the transmission and the reflection gratings. For Bragg angles such that $\theta < \theta_D{}^T$, $\alpha_2 > 0$, the transmission grating exhibits normal dispersion. For Bragg angles such that $45° < \theta < \theta_D{}^R$, $\beta_2 > 0$, the reflection grating exhibits normal dispersion. In the normal-dispersion regime the higher-frequency components of an optical pulse travels slower than its lower frequency components. By contrast, the opposite occurs in the anomalous-dispersion regime in which $\alpha_2 < 0 (\beta_2 < 0)$.

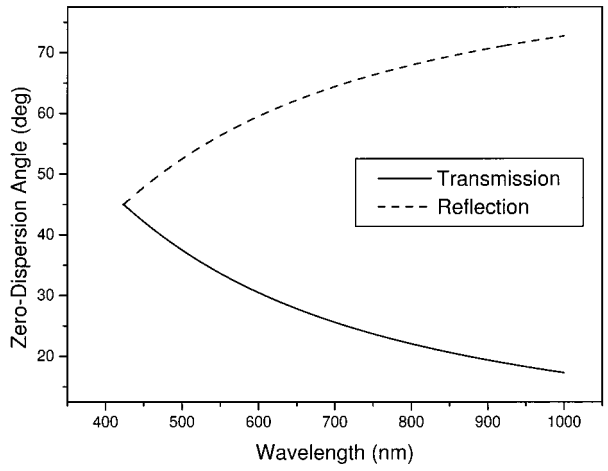

Fig. 9. Zero-dispersion angle versus wavelength. Solid and dashed curves represent the transmission grating and the reflection grating, respectively.

In all the calculations presented here we neglected the third and higher orders. If we, however, consider them here in the transmission-grating case, the ratio of the third- and second-order term in the expansion of $\Delta\alpha$ is given by[2]

$$R_P = \left|\frac{\alpha_3(\Omega - \omega_l)^3}{\alpha_2(\Omega - \omega_l)^2}\right| \approx \left|\frac{\sin^2\theta}{k\cos^2\theta}\left(\frac{\mathrm{d}k}{\mathrm{d}\Omega}\right) \times \left[1 + \frac{(\mathrm{d}k/\mathrm{d}\Omega)^2/k}{\sin^2\theta(\mathrm{d}k/\mathrm{d}\Omega)^2/k\cos^2\theta - (\mathrm{d}^2k/\mathrm{d}\Omega^2)}\right]\right| \times |\Delta\omega_l|, \tag{30}$$

where $|\Omega - \omega_l|$ has been approximated by the spectral width of the pulse $\Delta\omega_l$ and $|\Delta\omega_l| = (2\pi c)|\Delta\lambda_l|/\lambda_l{}^2$. We note that both the pulse characteristics (relative spectral width) and the crystal parameters determine the value of R_P. For 100-fs pulses we find that $R_P \approx 0.05$ and 0.03 at 450 and 800 nm, respectively. It is therefore justifiable to neglect the third- and higher-order dispersion. However, for 20-fs pulses, $R_P \approx 0.3$ and 0.14 at 450 and 800 nm, respectively. The analysis of short (<20-fs) femtosecond SPPC's requires therefore inclusion of both the third- and the higher-order dispersion in expanding $\Delta\alpha$ and $\Delta\beta$. This correction is also necessary when the Bragg angle approaches the zero-dispersion angle. The valid regime for the RG- and $2k$-grating-based SPPCM can be shown as the same as that for the TG-SPPCM.

In conclusion, we have studied the temporal characteristics of phase-conjugate pulse generated in self-pumped phase-conjugate geometries with either transmission- or reflection-grating dominated regimes. We showed that the second-order dispersion of the grating and the angular dispersion combine to compensate for the intrinsic dispersion of the crystal. When the compensation is complete, the SPPC pulse has a minimum pulse width, which is determined by the first-order dispersion of the grating. The SPPC of chirped pulse becomes transform limited and can be compressed compared with the pump pulse. The SPPC pulses are upchirped (downchirped) when the overall dispersion of the SPPCM is positive (negative). Our results also show that regions of anomalous dispersion exist for transmission gratings when the Bragg angle exceeds $\theta_D{}^T (\theta_D{}^T < \theta < 45°)$ and for reflection gratings when $45° < \theta < \theta_D{}^R$. We also demonstrated that for short (<20-fs) femtosecond pulses the present method should include the cubic- and the higher-order dispersion terms.

Phase conjugation has a range of applications in optical information processing and midband dispersion compensation in long-haul optical-fiber transmission. SPPC with short pulses in photorefractive materials has been successfully used for dynamic pulse holography and storage.[33,34] The simple and analytical approach we provided here can be used in these applications to aid the steady-state and linear analysis of temporal characteristics of SPPC.

ACKNOWLEDGMENTS

Changxi Yang and Min Xiao acknowledge the financial support provided by the U.S. National Science Foundation (grant EPS-9871977) and by the Office of Naval Research. M. Kaczmarek is grateful for the financial support of the Royal Society and the Engineering and Physical Sciences Research Council under grant GR/M/11844.

REFERENCES

1. See, for example, G. P. Agrawal, *Nonlinear Fiber Optics* (Academic, San Diego, Calif., 1995), and references therein.
2. See, for example, J. C. Diels and W. Rudolph, *Ultrashort Laser Pulse Phenomena: Fundamentals, Techniques, and Applications on Femtosecond Time Scale* (Academic, San Diego, Calif., 1995).
3. G. P. Agrawal, "Far-field diffraction of pulsed optical beams in dispersive media," Opt. Commun. **167**, 15–22 (1999).
4. H. A. Haus and W. S. Wong, "Solitons in optical communications," Rev. Mod. Phys. **68**, 423–444 (1996).
5. C. M. de Sterke, N. G. R. Broderick, B. J. Eggleton, and M. J. Steel, "Nonlinear optics in fiber gratings," Opt. Fiber Technol. Mater. Devices Syst. **2**, 253–268 (1996).
6. T. G. Brown and B. J. Eggleton, "Focus issue: Bragg solitons and nonlinear optics of periodic structures," Opt. Express **3**, 384–476 (1998).
7. N. G. Broderick, D. Taverner, D. J. Richardson, M. Ibsen, and R. I. Laming, "Optical pulse compression in fiber Bragg gratings," Phys. Rev. Lett. **79**, 4566–4569 (1997).
8. F. Ouellete, "Dispersion cancellation using linearly chirped Bragg grating filters in optical waveguides," Opt. Lett. **12**, 847–849 (1987).
9. F. Ouellette, "Limits of chirped pulse compression with an unchirped Bragg grating filter," Appl. Opt. **29**, 4826–4829 (1990).
10. B. J. Eggleton, C. M. de Sterke, and R. E. Slusher, "Nonlinear pulse propagation in Bragg gratings," J. Opt. Soc. Am. B **14**, 2980–2993 (1997).
11. G. Lenz, B. J. Eggleton, and L. Litchinitser, "Pulse compression using fiber gratings as highly dispersive nonlinear elements," J. Opt. Soc. Am. B **15**, 715–721 (1998).
12. H. G. Winful, "Pulse compression in optical fiber filters," Appl. Phys. Lett. **46**, 527–529 (1985).
13. P. St. J. Russell, "Bloch wave analysis of dispersion and pulse propagation in pure distributed feedback structures," J. Mod. Opt. **38**, 1599–1619 (1991).
14. B. J. Eggleton, R. E. Slusher, C. M. de Sterke, P. A. Krug, and J. E. Sipe, "Bragg grating solitons," Phys. Rev. Lett. **76**, 1627–1630 (1996).
15. B. J. Eggleton, G. Lenz, R. E. Slusher, and N. M. Litchinitser, "Compression of optical pulses spectrally broadened by self-phase modulation with a fiber Bragg grating in transmission," Appl. Opt. **37**, 7055–7061 (1998).
16. A. Pecchia, M. Laurito, P. Apai, and M. B. Danailov, "Studies of two-wave mixing of very broad-spectrum laser light in $BaTiO_3$," J. Opt. Soc. Am. B **16**, 917–923 (1999).
17. L. H. Aciolo, M. Ulman, E. P. Ippen, J. G. Fujimoto, H. Kong, B. S. Chen, and M. Cronin-Golomb, "Femtosecond temporal encoding in barium titanate," Opt. Lett. **16**, 1984–1986 (1991).
18. H. F. Yau, P. J. Wang, E. Y. Pan, and J. Chen, "Self-pumped phase conjugation with femtosecond pulses by use of $BaTiO_3$," Opt. Lett. **21**, 1168–1170 (1996).
19. H. F. Yau, P. J. Wang, E. Y. Pan, J. Chen, and J. Y. Chang, "Self-pumped phase conjugation with picosecond and femtosecond pulses using $BaTiO_3$," Opt. Commun. **135**, 331–336 (1997).
20. C. Yang, K. Minoshima, K. Seta, H. Matsumoto, and Y. Zhu, "Generation of self-pumped phase conjugation from the $-c$-face of $BaTiO_3$ with femtosecond pulses," Appl. Opt. **38**, 1704–1708 (1999).
21. C. Yang, K. Minoshima, K. Seta, and H. Matsumoto, "Characterization of femtosecond self-pumped phase conjugation in $BaTiO_3$," Appl. Phys. Lett. **74**, 2062–2064 (1999).
22. C. Yang, "Propagation and self-pumped phase conjugation of femtosecond laser pulses in $BaTiO_3$," J. Opt. Soc. Am. B **16**, 871–877 (1999).
23. M. B. Danailov, K. Diomande, P. Apai, and R. Szipocs, "Phase conjugation of broadband laser pulses in $BaTiO_3$," J. Mod. Opt. **45**, 5–9 (1998).
24. A. Yariv, D. Fekete, and D. M. Pepper, "Compensation for channel dispersion by nonlinear optical phase conjugation," Opt. Lett. **4**, 52–54 (1979).
25. S. X. Dou, M. Chi, H. Song, X. Zhang, Y. Zhu, and P. Ye, "Effect of reflection and $2K$ gratings on self-pumped phase-conjugate mirrors: theoretical and experimental studies," J. Opt. Soc. Am. B **16**, 428–434 (1999).
26. J. Feinberg, "Self-pumped, continuous-wave phase conjugation using internal reflection," Opt. Lett. **7**, 486–488 (1982).
27. N. V. Kukhtarev, T. I. Semenets, K. H. Ringhofer, and G. Tomberger, "Phase conjugation by reflection grating in electro-optic crystals," Appl. Phys. B **41**, 259–263 (1986).
28. K. Nakagawa, M. Zgonik, and P. Gunter, "Reflection gratings in self-pumped phase-conjugate mirrors," J. Opt. Soc. Am. B **14**, 839–845 (1997).
29. S. H. Lin, Y. W. Lian, P. Yeh, K. Hsu, and Y. Zhu, "$2k$-grating-assisted self-pumped phase conjugation: theoretical and experimental studies," J. Opt. Soc. Am. B **13**, 1772–1779 (1996).
30. P. Yeh, *Introduction to Photorefractive Nonlinear Optics* (Wiley, New York, 1993), Chap. 2.
31. C. Yang, "Dispersion compensation for a femtosecond self-pumped phase conjugator," Opt. Lett. **24**, 31–33 (1999).
32. K. Buse, S. Riehemann, S. Loheide, H. Hesse, F. Mersch, and E. Kratzig, "Refractive-indexes of single domain $BaTiO_3$ for different wavelengths and temperatures," Phys. Status Solidi A **135**, K87–K89 (1993).
33. Y. Ding, D. D. Nolte, M. R. Melloch, and A. M. Weiner, "Time-domain image processing using dynamic holography," IEEE J. Sel. Top. Quantum Electron. **4**, 332–341 (1998).
34. K. Oba, P. C. Sun, and Y. Fainman, "Nonvolatile photorefractive spectral holography," Opt. Lett. **23**, 915–917 (1998).